Event-Triggered Pose Synchronization in SE(3) for Cooperating Multi-Robot Teams

Pablo Budde gen. Dohmann * **Sandra Hirche** *

* *Chair of Information-oriented Control, Technical University of Munich, 80333 Munich, Germany (e-mail: {pablo.dohmann, hirche}@tum.de).*

Abstract: Consensus and synchronization are fundamental concepts for the coordination of cooperating multi-robot teams. Applications like cooperative manipulation may require not only synchronization of the position, but also of the orientation of the individual agents. The pose of the agent can be described within the special Euclidean group and common results for coordination have to be adapted. We propose a control framework for full-pose synchronization in $SE(3)$ for a team of Euler-Lagrange agents, relying only on relative information in the absence of a global coordinate frame. The framework consists of an inner loop for feedback linearization and an outer loop for pose synchronization. The measurements are taken by external sensors and communicated to the respective agents via a common communication network. To deal with limited communication bandwidth, we propose an event-triggered update strategy for the relative measurements. Finally, the efficacy of the proposed control and triggering law is illustrated in simulations.

Keywords: Event-triggered and self-triggered control, Networked robotic systems, Multi-agent systems, Consensus, Networked robotic system modeling and control

1. INTRODUCTION

The recent successes in communication technology enable distributed multi-agent coordination over wireless communication networks, with applications in manufacturing, search and rescue and surveillance (Roumeliotis and Bekey, 2002; Montijano et al., 2016). Especially, consensus and synchronization of the individual agents states is a fundamental task in multi-agent coordination problems like cooperative manipulation (B. gen. Dohmann and Hirche, 2020b). In such settings, the communication bandwidth is typically limited and, as a result, high network traffic can lead to negative effects like delays and packet dropout. Since typically continuous control laws are approximated by discrete systems with high sampling intervals, those constraints can not be maintained, and it becomes crucial to limit the amount of networked data. In order to reduce the network traffic, event-triggered control presents a promising alternative and several single and multi-agent problems have already been solved in event-triggered fashion (Heemels et al., 2012; Tabuada, 2007; Dimarogonas et al., 2012; B. gen. Dohmann and Hirche, 2020a; Liu et al., 2014). While event-triggered attitude synchronization exists (Weng and Yue, 2016), those rely on absolute measurements in a common inertial frame and disregard the position of the agents. However, in many real-world scenarios a common reference frame is unavailable and pose synchronization, with only relative measurements, becomes of great interest. Time-continuous control frameworks for the relative pose synchronization problem in $SE(3)$ exist, considering simple first order models (Hatanaka et al., 2012). In (Thunberg et al., 2016) the authors present pose-synchronization control laws for a group of agents, modeled by first and second order systems. The results are general in the sense that they cover relative and absolute measurements, as well as different types for the representation of the orientation. Local stability results are provided for all presented cases; depending on the type of controller used, different assumptions on the initial angle of rotation are required. For applications in robotics these results need to be adapted, considering the well known Euler-Lagrange equations commonly used to model mechanical systems. To the best knowledge of the authors an event-triggered framework for full-pose synchronization in the absence of a common inertial frame is non-existent in this context.

In this work we present a control framework for pose synchronization for Euler-Lagrange agents, consisting of a local control loop for feedback linearization, combined with an external control loop for the synchronization task. The external loop relies solely on relative measurements, which are obtained from external sensing agents and communicated in event-triggered fashion. Our existing works show how event-triggered control can reduce the load on the communication drastically and that tasks such as cooperative manipulation can benefit from position synchronization (B. gen. Dohmann and Hirche, 2020b,a). However, they only deal with synchronization of the translational position and joint states, respectively. The contribution of this work is to provide an event-triggered control algo-

⋆ This work was supported by the German Research Foundation (DFG) within the Joint Sino-German research project Control and Optimization for Event-triggered Networked Autonomous Multi-agent Systems (COVEMAS).

©2023 the authors. This work has been accepted to IFAC for publication under a Creative Commons Licence CC-BY-NC-ND.

rithm for *full pose* synchronization in $SE(3)$ using relative measurements only.

The remainder of the paper is structured as follows. In Section 2 we present some preliminaries, the agent model and the problem statement. In Section 3 we present the main control framework and the corresponding stability results. In Section 4 the results are illustrated in simulations and concluding remarks are provided in Section 5.

2. PRELIMINARIES AND PROBLEM STATEMENT

In this section we give a brief overview of our model and state the given problem.

2.1 Notation

Throughout this work, we denote with $\mathbf{0}$ a zero vector or matrix, whose dimensions are clear from context. For any $\boldsymbol{a} = [a_1 \ a_2 \ a_3]^T, a_k \in \mathbb{R}, \forall k \in \{1,2,3\}$, the operator $(\cdot)^\wedge : \mathbb{R}^3 \to so(3)$ is defined as

$$\boldsymbol{a}^\wedge = \begin{bmatrix} 0 & -a_3 & a_2 \\ a_3 & 0 & -a_1 \\ -a_2 & a_1 & 0 \end{bmatrix}, \tag{1}$$

where $so(3)$ corresponds to the vector space of all 3×3 skew-symmetric matrices. For any time-dependent variable $\boldsymbol{a}(t)$, we omit the time-dependency t if it is clear from context. The Euclidean norm of a vector and the matrix norm, induced by the Euclidean norm, are denoted by $\|(\cdot)\|_2$. The $\mathcal{L}_2$ and $\mathcal{L}_\infty$ norm of a function are denoted with $\|(\cdot)\|_{\mathcal{L}_2}$ and $\|(\cdot)\|_\infty$, respectively, and we say that a function is in $\mathcal{L}_2$ or $\mathcal{L}_\infty$ if the corresponding norm is bounded. The superscript $(\cdot)^l, \forall l \in \{z, r\}$ of any quantity refers to the translational and rotational degrees of freedom, respectively.

2.2 Graph Theory

We consider a team of N agents, which obtain relative measurements by a group of external sensors. The sensing topology of the sth sensor is described by the graph $\mathcal{G}_s = \{\mathcal{V}_s, \mathcal{E}_s\}$, where $\mathcal{V}_s \subseteq \{1, ..., N\}$ is the vertex set, representing the individual agents whose states can be sensed by s and $\mathcal{E} \subseteq \mathcal{V} \times \mathcal{V}$ is the edge set, where $(i,j) \in \mathcal{E}_s$ if sensor s can measure the relative pose of i and j. We consider that the complete sensing graph $\mathcal{G} = \bigcup_s \mathcal{G}_s = \{\mathcal{V}, \mathcal{E}\}$ is undirected, i.e. if $(i,j) \in \mathcal{E} \Rightarrow (j,i) \in \mathcal{E}$. The neighborhood of agent i is then defined as $N_i = \bigcup_s \{j \in \mathcal{V}_s | (i,j) \in \mathcal{E}_s\}$. Additionally, we pose the following assumption on the sensing topology.

Assumption 1.

(1) The complete sensing graph $\mathcal{G} = \bigcup_s \mathcal{G}_s$ is connected.

(2) If agent i receives a measurement of sensor s, its complete neighborhood has to be included in the sensing graph of s, i.e. $j \in \mathcal{V}_s, \forall j \in N_i$.

The first assumption is to ensure that the overall topology is connected, while the second assumption implies that the neighborhood N_i of each agent i is limited to the sensing range $\mathcal{V}_s$ of the sth sensor.

2.3 Rigid Body Motion

In this work we consider agents moving in the three-dimensional space, and we briefly introduce the basic concepts of rigid body motion. Each agent has a body-fixed coordinate frame Σ_i, the pose of which is represented with respect to the fixed inertial frame Σ_w by the homogeneous transformation matrix

$$\boldsymbol{g}_i = \begin{bmatrix} \boldsymbol{R}_i & \boldsymbol{p}_i \\ \mathbf{0} & 1 \end{bmatrix}, \tag{2}$$

where $\boldsymbol{p}_i \in \mathbb{R}^3$ is the translation and $\boldsymbol{R}_i \in SO(3)$ is the rotation of the frame Σ_i relative to the fixed inertial coordinate frame Σ_w. Define the body twist as $\boldsymbol{u}_i = \begin{bmatrix} \boldsymbol{v}_i^T & \boldsymbol{\omega}_i^T \end{bmatrix}^T \in \mathbb{R}^6$, where $\boldsymbol{v}_i, \boldsymbol{\omega}_i \in \mathbb{R}^3$ are the instantaneous linear and angular velocity. Differentiating (2) with respect to time, results in the well known kinematics

$$\dot{\boldsymbol{g}}_i = \begin{bmatrix} \boldsymbol{R}_i \boldsymbol{\omega}_i^\wedge & \boldsymbol{R}_i \boldsymbol{v}_i \\ \mathbf{0} & \mathbf{0} \end{bmatrix}. \tag{3}$$

The relative pose of agent j with respect to agent i is given as

$${}^i\boldsymbol{g}_j = \boldsymbol{g}_i^{-1} \boldsymbol{g}_j = \begin{bmatrix} {}^i\boldsymbol{R}_j & {}^i\boldsymbol{p}_j \\ \mathbf{0} & 1 \end{bmatrix}, \tag{4}$$

where ${}^i\boldsymbol{R}_j = \boldsymbol{R}_i^T \boldsymbol{R}_j$ and ${}^i\boldsymbol{p}_j = \boldsymbol{R}_i^T (\boldsymbol{p}_j - \boldsymbol{p}_i)$, with relative kinematics

$${}^i\dot{\boldsymbol{g}}_j = {}^i\boldsymbol{g}_j \begin{bmatrix} {}^j\boldsymbol{\omega}_i^\wedge & {}^j\boldsymbol{v}_i \\ 0 & 0 \end{bmatrix} \tag{5}$$

where the relative velocity is given as

$${}^j\boldsymbol{u}_i = \begin{bmatrix} {}^j\boldsymbol{v}_i \\ {}^j\boldsymbol{\omega}_i \end{bmatrix} = \boldsymbol{u}_j - \mathbf{Ad}_{({}^j\boldsymbol{g}_i)} \boldsymbol{u}_i \tag{6}$$

with the adjoint transformation

$$\mathbf{Ad}_{(\boldsymbol{g})} = \begin{bmatrix} \boldsymbol{R} & \boldsymbol{p}^\wedge \boldsymbol{R} \\ \mathbf{0} & \boldsymbol{R} \end{bmatrix} \forall \boldsymbol{g} = (\boldsymbol{R}, \boldsymbol{p}) \in SE(3). \tag{7}$$

Other representations of the orientation of agent i include the axis angle representation with the rotation axis $\{\boldsymbol{x}_i \in \mathbb{R}^3 | \ \|\boldsymbol{x}_i\|_2 = 1\}$ and rotation angle $\theta_i \in [0, \pi]$, as well as the unit quaternion $\boldsymbol{q}_i$ defined as

$$\boldsymbol{q}_i = \begin{bmatrix} \varepsilon_i \\ \boldsymbol{\eta}_i \end{bmatrix} = \begin{bmatrix} \cos(\theta_i/2) \\ \sin(\theta_i/2) \boldsymbol{x}_i \end{bmatrix}, \tag{8}$$

with corresponding time-derivative

$$\dot{\boldsymbol{q}}_i = \frac{1}{2} \begin{bmatrix} -\boldsymbol{\eta}_i^T \boldsymbol{\omega}_i \\ \varepsilon_i \boldsymbol{\omega}_i + \boldsymbol{\omega}_i^\wedge \boldsymbol{\eta}_i \end{bmatrix}. \tag{9}$$

2.4 Problem Statement

In this work we present a nested loop control framework for pose synchronization of N agents. The proposed control structure can be found in Figure 1. The dynamics of the ith agent are modeled using the well known Euler-Lagrange equations of motion transformed into the task space, which can be found in any textbook about robotics, as

$$\boldsymbol{M}_i(\boldsymbol{r}_i) \dot{\boldsymbol{u}}_i + \boldsymbol{C}_i(\boldsymbol{r}_i, \dot{\boldsymbol{r}}_i) \boldsymbol{u}_i + \boldsymbol{h}_i^g(\boldsymbol{r}_i) = \boldsymbol{h}_i, \tag{10}$$

where $\boldsymbol{r}_i \in \mathbb{R}^{d_i}, \boldsymbol{h}_i \in \mathbb{R}^6$ are the generalized coordinates and forces of the ith agent and d_i is the number of generalized coordinates of the ith agent. The matrices $\boldsymbol{M}_i(\boldsymbol{r}_i), \boldsymbol{C}_i(\boldsymbol{r}_i, \dot{\boldsymbol{r}}_i) \in \mathbb{R}^{6 \times 6}$ denote the inertia and Coriolis/centrifugal matrix of the ith agent and $\boldsymbol{h}_i^g(\boldsymbol{r}_i) \in \mathbb{R}^6$

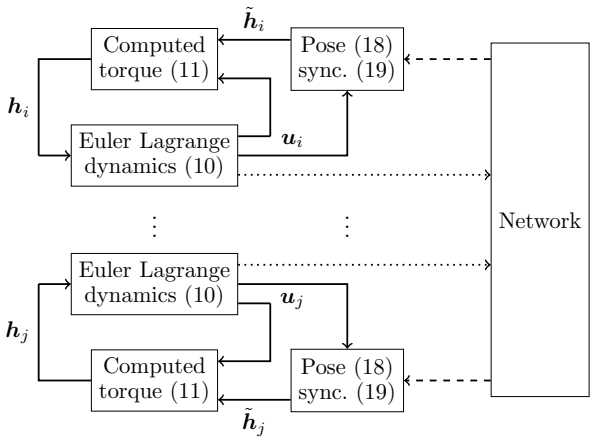

Fig. 1. Block diagram of the proposed control framework. The dotted lines correspond to continuous measurements of the agents pose and dashed lines correspond to event-triggered signals. The triggering condition can be evaluated directly at the sensors.

is the gravitation. With the well known computed torque approach

$$\boldsymbol{h}_i = \boldsymbol{C}_i(\boldsymbol{r}_i, \dot{\boldsymbol{r}}_i)\boldsymbol{u}_i + \boldsymbol{h}_i^g(\boldsymbol{r}_i) + \boldsymbol{M}_i(\boldsymbol{r}_i)\tilde{\boldsymbol{h}}, \tag{11}$$

where $\tilde{\boldsymbol{h}}_i = \begin{bmatrix}\boldsymbol{f}_i^T & \boldsymbol{\tau_i}\end{bmatrix}$ is an outer loop control law, we obtain the linearized dynamics as

$$\dot{\boldsymbol{v}}_i = \boldsymbol{f}_i \tag{12}$$
$$\dot{\boldsymbol{\omega}}_i = \boldsymbol{\tau}_i. \tag{13}$$

The outer loop consists of a control law for pose synchronization which is said to be achieved if $\forall i, j \in \mathcal{V}$

$$\|\boldsymbol{p}_i - \boldsymbol{p}_j\|_2 \to 0 \tag{14}$$
$$\left\|{}^i\boldsymbol{\eta}_j\right\|_2 \to 0. \tag{15}$$

Note that $\left\|{}^i\boldsymbol{\eta}_j\right\|_2 = 0$ iff $\boldsymbol{q}_i = \pm\boldsymbol{q}_j$, which means that agent i and j have the same orientation relative to a common frame. For achieving the control goal, each agent is assumed to have access only to relative pose information ${}^i\boldsymbol{p}_j, {}^i\boldsymbol{q}_j$ of its neighbors $j \in N_i$. We are interested in an event-triggered control law, which determines online the update instances of the control law, requiring only relative measurements. To solve the problem, we pose following assumptions on the initial angles of the rotations.

Assumption 2. For all agents $i \in \mathcal{V}$ the initial orientations satisfy $|\theta_i(0)| < \frac{\pi}{2}$.

Note that local stability results are quite common for control algorithms on $SE(3)$ and the posed assumption on the initial configuration is the same as for comparable time-continuous control approaches (Thunberg et al., 2016; Hatanaka et al., 2012).

Remark 1. The presented second order model is a common occurrence after feedback linearization of Euler-Lagrange systems. In case of model uncertainties, adaptive control approaches (Slotine and Li, 1987; Umlauft and Hirche, 2019) can be used and also integrated in even-triggered fashion (Liu et al., 2016).

3. OUTER LOOP POSE SYNCHRONIZATION

In this section we derive the outer loop for pose synchronization as well as the triggering condition, which determines online if data should be transmitted, in order to achieve stability of the complete system.

3.1 Control Law and Trigger Condition

We proceed by deriving a control law, which force the dynamics on a manifold where the sliding variables

$$\boldsymbol{s}_i = \boldsymbol{v}_i - \sum_{j\in N_i} k_{ij}^z\, {}^i\boldsymbol{p}_j \tag{16}$$
$$\boldsymbol{\varsigma}_i = \boldsymbol{\omega}_i - \sum_{j\in N_i} k_{ij}^r\, {}^i\boldsymbol{\eta}_j \tag{17}$$

are zero. On this manifold the remaining first order dynamics yield convergence of the relative pose error. For this consider the piecewise-continuous control inputs

$$\begin{aligned}\boldsymbol{f}_i(t) = &\sum_{j\in N_i} k_{ij}^z\, {}^i\dot{\boldsymbol{p}}_j(t_{k_{ij}}^z) \\ &- \frac{k_i^z}{m_i^z}\left(\boldsymbol{v}_i(t) - \sum_{j\in N_i} k_{ij}^z\, {}^i\boldsymbol{p}_j(t_{k_{ij}}^z)\right)\end{aligned} \tag{18}$$

$$\begin{aligned}\boldsymbol{\tau}_i(t) = &\sum_{j\in N_i} k_{ij}^r\, {}^i\dot{\boldsymbol{\eta}}_j(t_{k_{ij}}^r) \\ &- \frac{k_i^r}{m_i^r}\left(\boldsymbol{\omega}_i(t) - \sum_{j\in N_i} k_{ij}^r\, {}^i\boldsymbol{\eta}_j(t_{k_{ij}}^r)\right),\end{aligned} \tag{19}$$

where the gains $m_i^z, m_i^r, k_i^z, k_i^r, k_{ij}^z, k_{ij}^r > 0$. The trigger instances $t_{k_{ij}}^l, l \in \{z, r\}$ are defined as

$$t_{k_{ij}+1}^l = \inf\{t > t_{k_{ij}}^l | {}^i\mu_j^l + \phi_{ij}^l f_{ij}^l \le 0\} \tag{20}$$

where $\phi_{ij}^l > 0$, with the triggering functions

$$f_{ij}^t = \sigma_{ij}^z k_i^z \|\boldsymbol{s}_i\|_2^2 - \frac{1}{4\sigma_{ij}^z k_i^z}\left\|{}^i\boldsymbol{e}_j\right\|_2^2 \tag{21}$$

$$f_{ij}^r = \sigma_{ij}^r k_i^r \|\boldsymbol{\varsigma}_i\|_2^2 - \frac{1}{4\sigma_{ij}^r k_i^r}\left\|{}^i\boldsymbol{\zeta}_j\right\|_2^2, \tag{22}$$

where $0 < \sigma_{ij}^l, \quad \sigma_i^l = \sum_{j\in N_i}\sigma_{ij}^l < 0.5$, Finally, the trigger-induced errors are defined as

$${}^i\boldsymbol{e}_j = k_{ij}^z\left({}^i\dot{\boldsymbol{p}}_j(t) - {}^i\dot{\boldsymbol{p}}_j(t_{k_{ij}}^z)\right) + \frac{k_i^z k_{ij}^z}{m_i^z}\left({}^i\boldsymbol{p}_j(t) - {}^i\boldsymbol{p}_j(t_{k_{ij}}^z)\right) \tag{23}$$

$${}^i\boldsymbol{\zeta}_j = k_{ij}^r\left({}^i\dot{\boldsymbol{\eta}}_j(t) - {}^i\dot{\boldsymbol{\eta}}_j(t_{k_{ij}}^r)\right) + \frac{k_i^r k_{ij}^r}{m_i^r}\left({}^i\boldsymbol{\eta}_j(t) - {}^i\boldsymbol{\eta}_j(t_{k_{ij}}^r)\right) \tag{24}$$

and ${}^i\mu_j^l$ are the states of the dynamical systems

$${}^i\dot{\mu}_j^l(t) = -\alpha_{ij}^l\, {}^i\mu_j^l + f_{ij}^l \tag{25}$$

with initial condition ${}^i\mu_j^l(0) > 0$ and gain $\alpha_{ij}^l > 0$. Note that due to Assumption 1.2 each sensor has the available information to evaluate the trigger conditions locally. The following lemma about the properties of ${}^i\mu_j^l$ is crucial for the later analysis.

Lemma 1. ((Girard, 2015)). If for $l \in \{z, r\}$ the event-times $t_{k_{ij}}^l$ are chosen according to (20) and ${}^i\mu_j^l(0) > 0$, then ${}^i\mu_j^l(t) > 0, \forall 0 \le t < \infty$.

The proposed control law (18), (19) consists of a continuous feedback term of the velocities $\boldsymbol{v}_i, \boldsymbol{\omega}_i$, as well as a piecewise constant feedback of the triggered relative pose

and its derivative. The idea is that in situations where the relative states are measured by external sensors, those communicate their measurements to the agents over a wireless communication network. In such settings, efficient use of the communication bandwidth becomes crucial for the overall performance of the system. Note that $\boldsymbol{v}_i$ and $\boldsymbol{\omega}_i$ are the velocities in the body-fixed frame and thus can be locally measured by the agent itself and are not included in the event-triggering framework. The closed loop dynamics of the system are obtained, by substituting the control law (18), (19) into the linearized dynamics (12), (13) and using the definition of the trigger-induced error (23), (24), resulting in

$$m_i^z \dot{\boldsymbol{s}}_i + k_i^z \boldsymbol{s}_i + \sum_{j \in N_i} {}^i\boldsymbol{e}_j = \boldsymbol{0} \tag{26}$$

$$m_i^r \dot{\boldsymbol{\varsigma}}_i + k_i^r \boldsymbol{\varsigma}_i + \sum_{j \in N_i} {}^i\boldsymbol{\zeta}_j = \boldsymbol{0}. \tag{27}$$

Remark 2. For the sake of derivation, we assume scalar parameters $k_{ij}^z, k_{ij}^r, k_i^z, k_i^r, m_i^z, m_i^r$ for the control law. The results can be generalized using matrix-valued parameters, by adapting the presented Lyapunov functions.

3.2 Stability

We now present the main stability results of the proposed control law. We start by providing the following statement on the exponential decay of the sliding variables.

Lemma 2. The dynamics (26) and (27) are exponentially stable as

$$\|\boldsymbol{s}_i(t)\|_2^2 \leq \|W_i^z(0)\|_2^2 \exp\left(-\rho_i t\right) \tag{28}$$

$$\|\boldsymbol{\varsigma}_i(t)\|_2^2 \leq \|W_i^r(0)\|_2^2 \exp\left(-\varrho_i t\right), \tag{29}$$

where

$$\rho_i = \min\{(1-2\sigma_i^z)\,\frac{k_i^z}{m_i^z}, \sum_{j \in N_i} \alpha_{ij}^z\} \tag{30}$$

$$\varrho_i = \min\{(1-2\sigma_i^r)\,\frac{k_i^r}{m_i^r}, \sum_{j \in N_i} \alpha_{ij}^r\}. \tag{31}$$

Proof. Consider the Lyapunov candidates

$$W_i^t = \boldsymbol{s}_i^T m_i^z \boldsymbol{s}_i + \sum_{j \in N_i} {}^i\mu_j^z \tag{32}$$

$$W_i^r = \boldsymbol{\varsigma}_i^T m_i^z \boldsymbol{\varsigma}_i + \sum_{j \in N_i} {}^i\mu_j^r \tag{33}$$

with time-derivatives

$$\dot{W}_i^t \leq -\boldsymbol{s}_i^T k_i^z \left(\boldsymbol{s}_i + \sum_{j \in N_i} {}^i\boldsymbol{e}_j\right) + \sum_{j \in N_i} {}^i\dot{\mu}_j^z \tag{34}$$

$$\dot{W}_i^t \leq (\sigma_i^z - 1)\, k_i^z \left\|\boldsymbol{s}_i\right\|_2^2 \tag{35}$$

$$+ \sum_{j \in N_i} \left[\frac{1}{4\sigma_{ij}^z k_i^z} \left\|{}^i\boldsymbol{e}_j\right\|_2^2 - \alpha_{ij}^z {}^i\mu_j^z + f_{ij}^z\right] \tag{36}$$

$$\leq (2\sigma_i^z - 1)\, k_i^z \left\|\boldsymbol{s}_i\right\|_2^2 - \sum_{j \in N_i} \alpha_{ij}^z {}^i\mu_j^z \tag{37}$$

$$\leq -\rho_i W_i^z, \tag{38}$$

due to (21) and Lemma 1. Analogously, it can be shown that

$$\dot{W}_i^r \leq -\varrho_i W_i^r. \tag{39}$$

Due to the exponential decay of the sliding variables in Lemma 2, we have the following invariance property.

Lemma 3. For any positive a, b such that $0 < a < b < \pi/2$ and $c > 0$, if $\varrho_i \geq \frac{2bc}{(b-a)}$, $\theta_i(0) < a$ and $W_i^r(0) < c$ it holds that $\theta_i(t) < b$ and $W_i^r(t) < c$.

Proof. Define the potential

$$W_i = \theta_i^2 = \theta_i^2 \boldsymbol{x}_i^T \boldsymbol{x}_i \tag{40}$$

and denote $i = \arg\max_k W_k$, as the agent with maximum energy at time t. Taking the derivative, we obtain

$$\dot{W}_i = \theta_i \boldsymbol{x}_i^T \boldsymbol{L} \boldsymbol{\omega}_i, \tag{41}$$

where $\boldsymbol{L} = \boldsymbol{I} + f\boldsymbol{x}_i^\wedge + h(\boldsymbol{x}_i^\wedge)^2$, with some scalar f, h and note that $\boldsymbol{x}_i^T \boldsymbol{L} = \boldsymbol{x}_i^T$ due to the skew symmetric matrix. Substituting (17), we obtain

$$\dot{W}_i = \theta_i \boldsymbol{x}_i^T \left(\sum_{j \in N_i} k_{ij}^r {}^i\boldsymbol{\eta}_j + \boldsymbol{\varsigma}_i\right) \tag{42}$$

$$\leq \theta_i \boldsymbol{x}_i^T \sum_{j \in N_i} k_{ij}^r {}^i\boldsymbol{\eta}_j + \theta_i \left\|\boldsymbol{\varsigma}_i\right\|_2 \tag{43}$$

$$= \sum_{j \in N_i} \theta_i k_{ij}^r \boldsymbol{x}_i^T (\varepsilon_i \boldsymbol{\eta}_j - \varepsilon_j \boldsymbol{\eta}_i) + \theta_i \left\|\boldsymbol{\varsigma}_i\right\|_2 \tag{44}$$

$$= \sum_{j \in N_i} \theta_i k_{ij}^r \left[\varepsilon_i \sin\left(\frac{\theta_j}{2}\right) \boldsymbol{x}_i^T \boldsymbol{x}_j - \varepsilon_j \sin\left(\frac{\theta_i}{2}\right)\right] \tag{45}$$

$$+ \theta_i \left\|\boldsymbol{\varsigma}_i\right\|_2 \tag{46}$$

$$\leq \sum_{j \in N_i} \theta_i k_{ij}^r \sin\left(\frac{\theta_j - \theta_i}{2}\right) + \theta_i \left\|\boldsymbol{\varsigma}_i\right\|_2 \tag{47}$$

$$\leq \theta_i \left\|\boldsymbol{\varsigma}_i\right\|_2 \leq \theta_i W_i^r(0) \exp\left(-\frac{\varrho_i}{2} t\right), \tag{48}$$

since $\theta_i \sin(\frac{\theta_j - \theta_i}{2}) \leq 0$ if $\theta_i > \theta_j$. Without loss of generality assume the initial time $t_0 = 0$ and considering θ_i is a continuous variable, there exists an interval $[0, t_1)$ such that

$$\dot{W}_i \leq bc \exp\left(-\frac{\varrho_i}{2} t\right). \tag{49}$$

The rest of the proof follows the lines of Proposition 26 in (Thunberg et al., 2016) and is omitted here.

With the presented results, we can finally state the main theorem of this work, regarding the overall stability of the system.

Theorem 1. If Assumptions 1 and 2 are fulfilled and the event-times are chosen according to (20), the dynamics (26) and (27) achieve pose synchronization asymptotically and the inter-event times are lower bounded as

$$t_{k_{ij}+1}^r - t_{k_{ij}}^r \geq \frac{1}{\tau} \frac{4\sigma_{ij}^r k_i^r}{\phi_{ij}^r} \left({}^i\mu_j^r + \sigma_{ij}^r k_i^r \left\|\boldsymbol{\varsigma}_i\right\|_2^2\right), \tag{50}$$

which is strictly positive for any finite time.

Proof. In the following we will prove the results for the more technically involved rotational case and remark that similar steps can be followed for the proof of the relative translation using the potential function

$$W^t = \frac{1}{2} \sum_{i=1}^{N} \left\|\boldsymbol{p}_i\right\|_2^2. \tag{51}$$

Now consider the potential

$$W^r = \sum_{i=1}^{N} \|\boldsymbol{\eta}_i\|_2^2 \tag{52}$$

with time-derivative

$$\dot{W}^r = \sum_{i=1}^{N} \varepsilon_i \boldsymbol{\eta}_i^T \boldsymbol{\omega}_i \tag{53}$$

$$= \sum_{i=1}^{N} \varepsilon_i \boldsymbol{\eta}_i^T \left(\sum_{j \in N_i} k_{ij}^r \, {}^i\boldsymbol{\eta}_j + \boldsymbol{\varsigma}_i \right) \tag{54}$$

$$\leq \sum_{i=1}^{N} \varepsilon_i \left[\boldsymbol{\eta}_i^T \sum_{j \in N_i} k_{ij}^r \, {}^i\boldsymbol{\eta}_j + \frac{e_1}{2} \left\| {}^i\boldsymbol{\eta}_j \right\|_2^2 + \frac{1}{2e_1} \|\boldsymbol{\varsigma}_i\|_2^2 \right],$$

where the last line follows from Young's inequality for any $0 < e_1$. In the appendix, we show that if $\theta_i \leq \frac{\pi}{2}$ for all agents and a balanced graph, there exists a $e_2 > 0$ such that

$$\sum_{i=1}^{N} \sum_{j \in N_i} \varepsilon_i \boldsymbol{\eta}_i^T \, {}^i\boldsymbol{\eta}_j \leq - \sum_{i=1}^{N} \sum_{j \in N_i} e_2 \left\| {}^i\boldsymbol{\eta}_j \right\|_2^2. \tag{55}$$

Thus, by integrating (53) in the time-interval $[0, t]$, we have

$$W^r(t) \leq W(0) \tag{56}$$

$$- \sum_{i=1}^{N} \sum_{j \in N_i} \int_0^t \left[(e_2 k_{ij}^r - \frac{e_1}{2}) \left\| {}^i\boldsymbol{\eta}_j \right\|_2^2 - \frac{1}{2e_1} \|\boldsymbol{\varsigma}_i\|_2^2 \right].$$

Note that due to Lemma 2, $\boldsymbol{\varsigma}_i \in \mathcal{L}_2, \mathcal{L}_\infty$. Additionally, there always exists an e_1 such that $e_1 < 2e_2 k_{ij}^r$. As a result, we can conclude that $-(e_2 k_{ij}^r - \frac{e_1}{2}) \left\| {}^i\boldsymbol{\eta}_j \right\|_2^2$ is negative definite. It follows that ${}^i\boldsymbol{\eta}_j \in \mathcal{L}_2, \mathcal{L}_\infty$ and considering (17), $\boldsymbol{\omega}_i \in \mathcal{L}_\infty$ and with that ${}^i\dot{\boldsymbol{\eta}}_j \in \mathcal{L}_\infty$ can be concluded. Local asymptotic stability then follows from Barbalat's Lemma and considering that the graph is connected. Regarding the minimum inter-event times, consider the time-interval $[t_{k_{ij}}^r, t_{k_{ij}+1}^r)$. The derivative of $\left\| {}^i\boldsymbol{\zeta}_j \right\|_2$ in the given interval is obtained as

$$\frac{d}{dt} \left\| {}^i\boldsymbol{\zeta}_j \right\|_2 \leq \left\| {}^i\dot{\boldsymbol{\zeta}}_j \right\|_2 \leq k_{ij}^r \left\| {}^i\ddot{\boldsymbol{\eta}}_j \right\|_2 + \frac{k_i^z k_{ij}^r}{m_i^r} \left\| {}^i\dot{\boldsymbol{\eta}}_j \right\|_2. \tag{57}$$

Note that with (9) and (27) it can be shown that all terms are bounded and as a result

$$\frac{d}{dt} \left\| {}^i\boldsymbol{\zeta}_j \right\|_2 \leq \tau \tag{58}$$

for some $\tau > 0$. By integration over $[t_{k_{ij}}^r, t]$ for any $t \in [t_{k_{ij}}^r, t_{k_{ij}+1}^r)$ we thus obtain

$$\left\| {}^i\boldsymbol{\zeta}_j(t) \right\|_2 - \left\| {}^i\boldsymbol{\zeta}_j(t_{k_{ij}}^r) \right\|_2 \leq \tau (t - t_{k_{ij}}^r) \tag{59}$$

Note that $\left\| {}^i\boldsymbol{\zeta}_j(t_{k_{ij}}^r) \right\|_2 = 0$ and by definition (20), it holds that

$$\lim_{t \to t_{k_{ij}+1}^r} \left\| {}^i\boldsymbol{\zeta}_j(t) \right\|_2 = \frac{4\sigma_{ij}^r k_i^r}{\phi_{ij}^r} ({}^i\mu_j^r + \sigma_{ij}^r k_i^r \|\boldsymbol{\varsigma}_i\|_2^2), \tag{60}$$

resulting in (50). Finally, since by Lemma 1 we have that ${}^i\mu_j^r > 0$ and, as a result, (50) is strictly positive for any finite time.

4. SIMULATIONS

In this section we perform simulations and provide illustrative results for the proposed control approach. We use the closed-loop dynamics (26) and (27), with $m_i^z = m_i^r = 1, k_i^z = k_i^r = k_{ij}^z = k_{ij}^r = 10$ and the event-times are determined via the triggering law (20), with $\phi_{ij}^l = \alpha_{ij}^l = 1, {}^i\mu_j(0) = 0.5, \sigma_{ij}^l = 0.4$ for $l \in \{z, r\}$. The initial configurations $\boldsymbol{p}_i(0), \theta_i(0)\boldsymbol{x}_i(0)$ of the agents are chosen as

$$\begin{aligned}
\boldsymbol{p}_1(0) &= [2\ 0\ 6]^T \\
\boldsymbol{p}_2(0) &= [4\ -2\ -4]^T \\
\boldsymbol{p}_3(0) &= [6\ 2\ 4]^T \\
\boldsymbol{p}_4(0) &= [-2\ -4\ 0]^T \\
\theta_1(0)\boldsymbol{x}_1(0) &= [0.21\ 0.5\ 0.77]^T \\
\theta_2(0)\boldsymbol{x}_2(0) &= [0.6\ 0.04\ 0.83]^T \\
\theta_3(0)\boldsymbol{x}_3(0) &= [-0.21\ 0.77\ -0.5]^T \\
\theta_4(0)\boldsymbol{x}_4(0) &= [-0.63\ 0.37\ -0.64]^T
\end{aligned}$$

and the initial velocities are chosen as $\boldsymbol{u}_i = \boldsymbol{0}$. We chose four sensing agents whose vertex set corresponds to the neighborhood of a respective agent as $\mathcal{V}_1 = N_1 = \{2, 4\}, \mathcal{V}_2 = N_2 = \{1, 3\}, \mathcal{V}_3 = N_3 = \{2, 4\}, \mathcal{V}_4 = N_4 = \{1, 3\}$. The duration of the simulation is 1s and the sampling frequency is chosen as 1kHz. Note that the bound in Lemma 2 and with that the conditions in Lemma 3 are quite conservative. We will see in the following that the convergence properties can still be maintained, even if the conditions are not met. The two top plots in Figure 2 show the potentials W^t and W^r as defined in (51) and (52). As it can be seen both potentials decrease, illustrating the results in Theorem 1. The two bottom plots

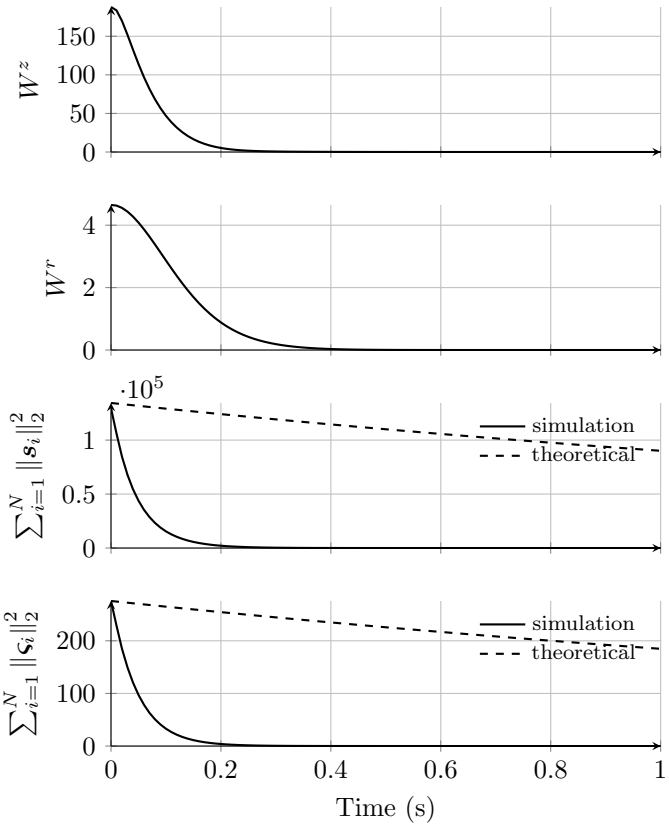

Fig. 2. Top: Tracking performance in terms of W^l for $l \in \{z, r\}$. Bottom: Tracking performance in terms of $\sum_{i=1}^{N} W_i^l$.

Table 1. Number of events between agent i and its first and second neighbor n_j^l for $j \in \{1,2\}$ translational ($l = z$) and rotational($l = r$) measurements, respectively.

i	n_1^z	n_2^z	n_1^r	n_2^r
1	22	19	26	48
2	23	17	18	35
3	14	27	47	22
4	23	26	34	18

Table 2. Minimum inter-event times between agent i and its first and second neighbor n_j^l for $j \in \{1,2\}$ translational ($l = z$) and rotational($l = r$) measurements, respectively.

i	n_1^z	n_2^z	n_1^r	n_2^r
1	0.01s	0.006s	0.01s	0.006s
2	0.015s	0.008s	0.015s	0.008s
3	0.006s	0.013s	0.006s	0.013s
4	0.008s	0.016s	0.008s	0.016s

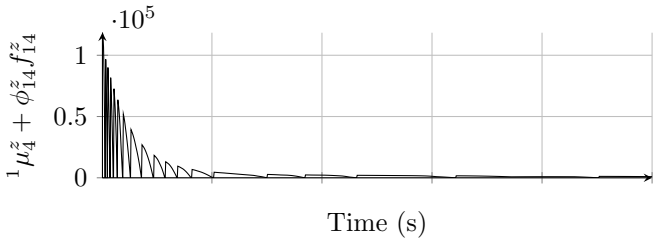

Fig. 3. Triggering-mechanism, illustrated as the triggering condition (20) for the translational measurement between agent 1 and 4.

of Figure 2 show the decay of the sum of the squared sliding variables $\sum_{i=1}^N \|\boldsymbol{s}_i\|_2^2$ and $\sum_{i=1}^N \|\boldsymbol{\varsigma}_i\|_2^2$ and the theoretical bound from Lemma 2, confirming the conservativeness of the results in the presented scenario. The result of the triggering is depicted in Table 1 with the number of events and in Table 2 with the minimum inter-event times. For reference, a periodic sampling scheme would result in 1000 transmissions. Immediately the efficiency of the proposed event-triggered framework can be seen with a drastic reduction in the transmission rates. In addition, since all minimum inter-event times are greater than 0.001s it can be concluded that no Zeno behavior was present during the simulations. Finally, in Figure 3 the trigger condition (20) for the relative translational measurements is provided. Recall that an event is triggered whenever zero is reached. It should be noted that at the start relative high trigger intervals are required, which become larger over the duration.

5. CONCLUSION

In this work we present a control law for pose synchronization in $SE(3)$ for a multi-robot team modeled with Euler-Lagrange equations. The control framework consists of a time-continuous inner control loop for feedback linearization, based only on locally available information and a piecewise continuous outer loop for the pose synchronization. In the absence of a common inertial frame, only relative measurements and local velocities are required for the outer loop. The relative poses are measured by external sensing agents, typically vision-based systems, and communicated to the respective agents. In order to reduce the load on the communication network, an event-triggered update strategy is used. We show that with the proposed event-triggering mechanism, the event instances are chosen such that asymptotic stability can be locally achieved. Finally, we conclude with simulations, illustrating the results. In the future we plan to include various network effects, such as delay and packet loss.

Appendix A. PROOF FOR INEQUALITY (55)

In the following we proof, that there exist an e_2, such that

$$\sum_{i=1}^N \sum_{j\in N_i} \varepsilon_i \boldsymbol{\eta}_i^{T\,i}\boldsymbol{\eta}_j + \sum_{i=1}^N \sum_{j\in N_i} e_2 \left\|{}^i\boldsymbol{\eta}_j\right\|_2^2 \leq 0 \tag{A.1}$$

Consider

$$\begin{aligned}
&\sum_{i=1}^N \sum_{j\in N_i} \varepsilon_i \boldsymbol{\eta}_i^{T\,i}\boldsymbol{\eta}_j + \sum_{i=1}^N \sum_{j\in N_i} e_2 \left\|{}^i\boldsymbol{\eta}_j\right\|_2^2 \\
&= \sum_{i=1}^N \sum_{j\in N_i} \left(\varepsilon_i^2 \boldsymbol{\eta}_i^T\boldsymbol{\eta}_j - \varepsilon_i\varepsilon_j \|\boldsymbol{\eta}_i\|_2^2 + e_2 \left\|{}^i\boldsymbol{\eta}_j\right\|_2^2\right) \\
&= \sum_{i=1}^N \sum_{j\in N_i} \Big(\varepsilon_i^2 \boldsymbol{\eta}_i^T\boldsymbol{\eta}_j - \varepsilon_i\varepsilon_j \|\boldsymbol{\eta}_i\|_2^2 \\
&\quad + e_2(\varepsilon_i^2 \|\boldsymbol{\eta}_j\|_2^2 + \varepsilon_j^2 \|\boldsymbol{\eta}_i\|_2^2 - 2\varepsilon_i\varepsilon_j \boldsymbol{\eta}_i^T\boldsymbol{\eta}_j + \|\boldsymbol{\eta}_i \times \boldsymbol{\eta}_j\|_2^2)\Big)
\end{aligned} \tag{A.2}$$

Considering that the graph is balanced, we can rewrite (A.2) as

$$\begin{aligned}
&\sum_{i=1}^N \sum_{j\in N_i} \Bigg[\frac{1}{2}\left(\varepsilon_i^2 + \varepsilon_j^2 - 4e_2\varepsilon_i\varepsilon_j\right)\boldsymbol{\eta}_i^T\boldsymbol{\eta}_j + e_2\|\boldsymbol{\eta}_i \times \boldsymbol{\eta}_j\|_2^2 \\
&- \left(\frac{1}{2}\varepsilon_i\varepsilon_j - e_2\varepsilon_i^2\right)\|\boldsymbol{\eta}_i\|_2^2 - \left(\frac{1}{2}\varepsilon_i\varepsilon_j - e_2\varepsilon_j^2\right)\|\boldsymbol{\eta}_i\|_2^2\Bigg]
\end{aligned} \tag{A.3}$$

Denoting $\angle(\boldsymbol{x}_i, \boldsymbol{x}_j)$ the angle between the $\boldsymbol{x}_i$ and $\boldsymbol{x}_j$ axis, we can rewrite the term

$$\begin{aligned}
&\frac{1}{2}\left(\varepsilon_i^2 + \varepsilon_j^2 - 4e_2\varepsilon_i\varepsilon_j\right)\boldsymbol{\eta}_i^T\boldsymbol{\eta}_j + e_2\|\boldsymbol{\eta}_i \times \boldsymbol{\eta}_j\|_2^2 \\
&= \frac{1}{2}\left(\varepsilon_i^2 + \varepsilon_j^2 - 4e_2\varepsilon_i\varepsilon_j\right)\sin(\theta_i/2)\sin(\theta_j/2)\cos(\angle(\boldsymbol{x}_i, \boldsymbol{x}_j)) \\
&+ e_2\sin^2(\theta_i/2)\sin^2(\theta_j/2)(1 - \cos^2(\angle(\boldsymbol{x}_i, \boldsymbol{x}_j))) \\
&\leq \frac{1}{2}\left(\varepsilon_i^2 + \varepsilon_j^2 - 4e_2\varepsilon_i\varepsilon_j\right)\sin(\theta_i/2)\sin(\theta_j/2)
\end{aligned}$$

for any $e_2 \leq \frac{\varepsilon_i^2+\varepsilon_j^2}{4\cos(\theta_i/2-\theta_j/2)}$. As such, the term in the sum (A.3) can be upper bounded as

$$\begin{aligned}
&\frac{1}{2}\left(\varepsilon_i^2 + \varepsilon_j^2 - 4e_2\varepsilon_i\varepsilon_j\right)\sin(\theta_i/2)\sin(\theta_j/2) \\
&- \left(\frac{1}{2}\varepsilon_i\varepsilon_j - e_2\varepsilon_i^2\right)\sin^2(\theta_j/2) - \left(\frac{1}{2}\varepsilon_i\varepsilon_j - e_2\varepsilon_j^2\right)\sin^2(\theta_i/2) \\
&= 2e_2\sin^2\left(\frac{\theta_j - \theta_i}{2}\right) - \frac{1}{2}\left(\sin(\theta_j) - \sin(\theta_i)\right)\sin\left(\frac{\theta_j - \theta_i}{2}\right),
\end{aligned}$$

where we use standard trigonometric identities. As a result,

$$2e_2\sin^2\left(\frac{\theta_j - \theta_i}{2}\right) - \frac{1}{2}\left(\sin(\theta_j) - \sin(\theta_i)\right)\sin\left(\frac{\theta_j - \theta_i}{2}\right) \leq 0$$

holds if

$$\Rightarrow e_2 \leq \frac{\sin(\theta_j) - \sin(\theta_i)}{4\sin\left(\frac{\theta_j - \theta_i}{2}\right)} = \frac{1}{2}\cos\left(\frac{\theta_i + \theta_j}{2}\right). \qquad \text{(A.4)}$$

As a result of Lemma 3 there always exists a strictly positive e_2 fulfilling (A.4).

REFERENCES

B. gen. Dohmann, P. and Hirche, S. (2020a). Event-triggered consensus for euler-lagrange systems with communication delay. *21st IFAC World Congress*, 53(2), 2777–2782.

B. gen. Dohmann, P. and Hirche, S. (2020b). Distributed control for cooperative manipulation with event-triggered communication. *IEEE T-RO*, 36(4), 1038–1052.

Dimarogonas, D.V., Frazzoli, E., and Johansson, K.H. (2012). Distributed event-triggered control for multi-agent systems. *IEEE TAC*, 57(5), 1291–1297.

Girard, A. (2015). Dynamic triggering mechanisms for event-triggered control. *IEEE TAC*, 60(7), 1992–1997.

Hatanaka, T., Igarashi, Y., Fujita, M., and Spong, M.W. (2012). Passivity-based pose synchronization in three dimensions. *IEEE TAC*, 57(2), 360–375.

Heemels, W.P.M.H., Johansson, K.H., and Tabuada, P. (2012). An introduction to event-triggered and self-triggered control. In *IEEE 51st CDC*, 3270–3285.

Liu, Q., Ye, M., Qin, J., and Yu, C. (2016). Event-based leader-follower consensus for multiple euler-lagrange systems with parametric uncertainties. In *IEEE 55th CDC*, 2240–2246.

Liu, Q., Wang, Z., He, X., and Zhou, D. (2014). A survey of event-based strategies on control and estimation. *Systems Science & Control Engineering*, 2(1), 90–97.

Montijano, E., Cristofalo, E., Zhou, D., Schwager, M., and Sagüés, C. (2016). Vision-based distributed formation control without an external positioning system. *IEEE T-RO*, 32(2), 339–351.

Roumeliotis, S.I. and Bekey, G.A. (2002). Distributed multirobot localization. *IEEE Transactions on Robotics and Automation*, 18(5), 781–795.

Slotine, J.J.E. and Li, W. (1987). On the adaptive control of robot manipulators. *IJRR*, 6(3), 49–59.

Tabuada, P. (2007). Event-triggered real-time scheduling of stabilizing control tasks. *IEEE TAC*, 52(9), 1680–1685.

Thunberg, J., Goncalves, J., and Hu, X. (2016). Consensus and formation control on SE(3) for switching topologies. *Automatica*, 66, 109–121.

Umlauft, J. and Hirche, S. (2019). Feedback linearization based on gaussian processes with event-triggered online learning. *IEEE TAC*, 65(10), 4154–4169.

Weng, S. and Yue, D. (2016). Distributed event-triggered cooperative attitude control of multiple rigid bodies with leader–follower architecture. *IJSS*, 47(3), 631–643.